ARMY RESEARCH LABORATORY

Microstructure, Fracture Characteristics, and Tensile Properties of Two Tungsten Heavy Alloys

Edward W. Kennedy

ARL-MR-269 November 1995

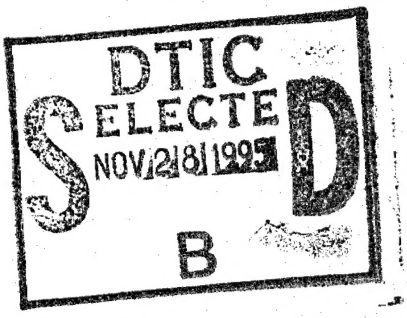

NOTICES

Destroy this report when it is no longer needed. DO NOT return it to the originator.

Additional copies of this report may be obtained from the National Technical Information Service, U.S. Department of Commerce, 5285 Port Royal Road, Springfield, VA 22161.

The findings of this report are not to be construed as an official Department of the Army position, unless so designated by other authorized documents.

The use of trade names or manufacturers' names in this report does not constitute indorsement of any commercial product.

REPORT DOCUMENTATION PAGE

Form Approved
OMB No. 0704-0188

1. AGENCY USE ONLY *(Leave blank)*	2. REPORT DATE	3. REPORT TYPE AND DATES COVERED
	November 1995	Final, January 1992–March 1993

4. TITLE AND SUBTITLE
Microstructure, Fracture Characteristics, and Tensile Properties of Two Tungsten Heavy Alloys

5. FUNDING NUMBERS
PR: 1L162618AH80

6. AUTHOR(S)
Edward W. Kennedy

7. PERFORMING ORGANIZATION NAME(S) AND ADDRESS(ES)
U.S. Army Research Laboratory
ATTN: AMSRL-WT-TC
Aberdeen Proving Ground, MD 21005-5066

8. PERFORMING ORGANIZATION REPORT NUMBER
ARL-MR-269

9. SPONSORING/MONITORING AGENCY NAME(S) AND ADDRESS(ES)

10. SPONSORING/MONITORING AGENCY REPORT NUMBER

11. SUPPLEMENTARY NOTES

12a. DISTRIBUTION/AVAILABILITY STATEMENT
Approved for public release; distribution is unlimited.

12b. DISTRIBUTION CODE

13. ABSTRACT *(Maximum 200 words)*

The influence of microstructure on fracture behavior and tensile properties was investigated for two tungsten heavy alloys (93W-4.9Ni-2.1Fe and 91W-6Ni-3Co by weight-percentage) that are suitable material candidates for use as kinetic energy penetrators. Both alloys were evaluated in swaged and aged conditions. For comparable levels of swaging and aging, the W-Ni-Co alloy exhibited increased tensile strength and ductility compared to the W-Ni-Fe material. The W-Ni-Co alloy had a smaller average W grain size and a larger percentage of W in the matrix. Fracture surfaces of failed uniaxial tensile specimens tested at quasi-static ($\dot{\varepsilon} = 10^{-4}\ s^{-1}$) and low-to-medium ($\dot{\varepsilon} = 10^{0}\ s^{-1}$) strain rates were characterized using scanning electron microscopy. The results indicate a strong relationship between microstructure, fracture behavior, and tensile properties as a function of alloy composition and strain rate.

14. SUBJECT TERMS
tungsten heavy alloy, tungsten-nickel-iron alloy, tungsten-nickel-cobalt alloy, microstructure, fracture characteristics, tensile properties, strain rate sensitivity, scanning electron microscopy, kinetic energy penetrators

15. NUMBER OF PAGES
29

16. PRICE CODE

17. SECURITY CLASSIFICATION OF REPORT	18. SECURITY CLASSIFICATION OF THIS PAGE	19. SECURITY CLASSIFICATION OF ABSTRACT	20. LIMITATION OF ABSTRACT
UNCLASSIFIED	UNCLASSIFIED	UNCLASSIFIED	UL

INTENTIONALLY LEFT BLANK.

ACKNOWLEDGMENTS

The author would like to acknowledge Mr. Gordon Dudder, Battelle Pacific Northwest Laboratories (BPNL), for conducting mechanical properties characterization; Mr. William Gurwell (BPNL) for providing insight on W heavy alloys; and Dr. Steve Caldwell, Teledyne Firth Sterling, for supplying the materials and sharing his knowledge on W heavy alloys. The author would also like to express his appreciation to Dr. Pat Kingman and Mr. Laszlo Kecskes, U.S. Army Research Laboratory (ARL), for assisting with scanning electron microscopy and Mr. Dwight Sheppard and Mr. Charles Klarich, U.S. Army Combat Systems Test Activity, for polishing and photographing optical microscopy samples. Mr. Brett Sorensen (ARL) provided kinetic energy projectile drawing.

INTENTIONALLY LEFT BLANK.

TABLE OF CONTENTS

INTENTIONALLY LEFT BLANK.

LIST OF FIGURES

LIST OF TABLES

INTENTIONALLY LEFT BLANK.

1. INTRODUCTION

Tungsten heavy alloys (WHAs) are multiphase materials containing 80–97 weight-percent tungsten (W) grains in a lower melting point metal matrix and are usually made by liquid-phase sintering a compact composed of elemental powders such as nickel (Ni), iron (Fe), and/or cobalt (Co). The as-sintered material is generally vacuum-annealed to remove trapped hydrogen, solution-heat-treated to homogenize the matrix, and then water-quenched to reduce segregation of impurities. Mechanical properties can be tailored for a specific end use by thermomechanical (TM) processing techniques. Swaging followed by an aging heat treatment increases tensile and compressive strengths of as-sintered materials, while maintaining moderate ductility. Heavy alloys with higher weight-percent W have a smaller volume of matrix. The result is increased contiguity between W grains, which makes the alloy more susceptible to brittle fracture by providing lower energy paths for cracks to propagate. For applications where a combination of strength and toughness is required, alloy composition and TM processing should be selected to ensure that the resulting microstructure minimizes contiguity.

This report examines the influence of microstructure on the fracture behavior and tensile properties of swaged and aged W-Ni-Fe and W-Ni-Co ternary alloys. Whereas the W-Ni-Fe system has been extensively studied, recent investigations indicate that W-Ni-Co alloys subjected to TM processing can attain excellent combinations of mechanical properties [1,2]. The W-Ni-Fe alloy was also studied in an as-sintered, vacuum-annealed, and solution-heat-treated condition (hereafter referred to as as-sintered). The fracture behavior of both alloys was assessed based on the surface characteristics of the broken ends of tensile specimens, which were tested in quasi-static and low-to-medium strain-rate ($\dot{\varepsilon}$) regimes. Correlations between microstructure, fracture behavior, and tensile properties are presented as a function of strain rate. Pertinent comments regarding the strain rate sensitivity of the two W heavy alloys are made. Applicability of the two WHAs for use as long rod kinetic energy (KE) penetrators is addressed.

2. BACKGROUND

Ramesh and Coates [4] recently provided a summary of appropriate literature on the correlation between TM processing history, microstructure, mechanical property response, and failure characteristics for heavy alloys of various W contents [5–8]. Research in the quasi-static strain rate regime indicates that the flow stress of as-sintered heavy alloys increases with W content [5,9]. Others have shown that such factors as mechanical working [2–4,7,9] and post-sintering and post-swaging heat treatments

[2,7,8,10,12–14] contribute to improved tensile strengths. Yet, alloys with increased tensile and compressive strengths generally show a concomitant reduction in ductility [5,6,11].

Investigators have shown that factors other than W content, such as matrix composition [2,15,16], impurity segregation [10,12,13,15–18], porosity [9,10,12,13], and intermetallics [12,17], influence the mechanical properties and fracture behavior of W heavy alloys. Extensive literature exists for W-Ni-Fe alloys which have a 7:3 ratio of Ni/Fe [3–14,16,19–21], as these materials can be manufactured to have good combinations of strength, toughness, and ductility and yet avoid the formation of brittle intermetallic phases [9]. Intermetallics and impurities at W-W interfaces and interphase regions between the matrix and W grains [12,17,18] have been shown to degrade strength and ductility as a result of intergranular fracture. Hydrogen embrittlement has been shown to severely reduce tensile properties at low strain rates [18].

WHAs generally fail by one or more of the following mechanisms [3,18–21]: intergranular fracture between W-W interfaces, fracture or decohesion along the W-matrix interface, intragranular cleavage and/or fracture of W grains, and/or failure by rupture of the matrix. The fracture mode is related to microstructural factors and the rate and nature of loading. Ductile fracture is characterized by intragranular cleavage of W grains. The matrix of an as-sintered W alloy is reasonably ductile and capable of being work-hardened, which tends to retard crack propagation [3,20]. However, high W content alloys (>93 weight-percent) tend to fracture in a brittle, intergranular manner as a result of increased contiguity between W grains [10–13], which provides a lower energy fracture path. Because WHAs are strain-rate sensitive (i.e., exhibit an increase in flow stress with increasing strain rate), a need exists to evaluate the mechanical behavior of W heavy alloys used in component designs that are subjected to elevated rates of strain, such as armor-piercing penetrators.

Studies have characterized the mechanical properties and fracture behavior of W heavy alloys at higher strain rates [3,4,8,21,22]. By developing a basic understanding of the relationship between microstructure and fracture behavior, a specific W heavy alloy can be manufactured to have mechanical properties that are suitable for the end-use design of the component. In some cases, it is desirable to produce a high-density W heavy alloy that has elevated tensile and compressive yield strengths, yet retains a reasonable degree of ductility. High strength and moderate ductility can be attained for heavy alloys with up to 93-weight-percent W [5], making such materials attractive for use as long rod KE penetrators used to defeat heavy armor.

The modern KE projectile fired from a main tank cannon consists of a subcaliber, fin-stabilized, long rod penetrator surrounded by a multisegment sabot. The primary function of the sabot is to ensure in-bore structural integrity of penetrator during launch. In addition, it must discard after exiting the gun muzzle in such a manner as to minimize aerodynamic disturbances that may affect the flight characteristics of the penetrator. The sabot should be designed to meet these requirements, while minimizing the parasitic weight of the projectile [23,24,25]. A typical KE projectile, with one sabot petal removed to expose the penetrator, is shown in Figure 1.

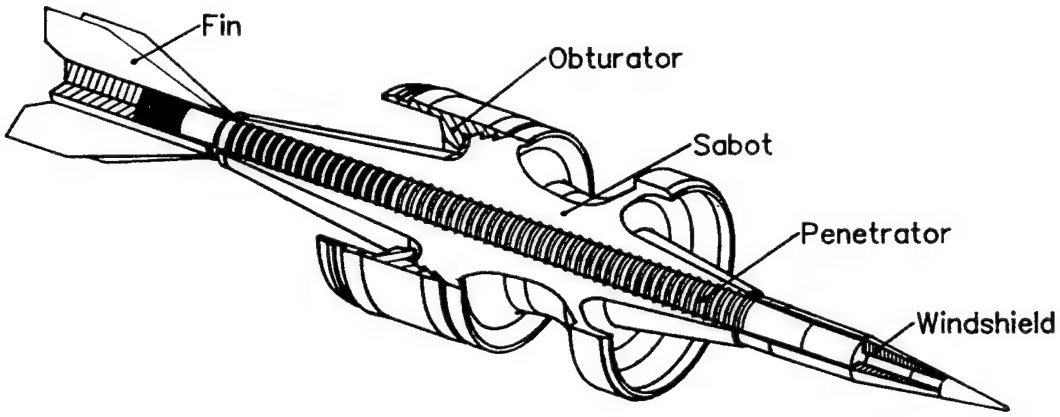

Figure 1. Typical KE projectile.

While the previously referenced studies have examined the mechanical properties of WHAs at strain rates in the 10^2- to 10^3-s^{-1} regime, the strain rates associated with a terminal ballistic event are on the order of 10^4 to 10^5 s^{-1}. Mechanical properties at these high rates of strain are of interest to those developing analytical and computational penetration mechanics models. Experimental studies have shown that the penetration performance of conventionally processed WHA penetrators into steel targets increases with density, yet does not exhibit a clear dependence upon increasing tensile and compressive properties [26,27]. However, mechanical properties and fracture characteristics will have a greater influence on the response and performance of long rod WHA penetrators vs. advanced armor combinations, which subject the penetrator to transverse loading. Such armor systems are generally positioned on armored vehicles at high obliquities, introducing a complex three-dimensional loading condition on the rod during the penetration process. Yet, the penetrator first experiences dynamic loading conditions during launch and flight.

Mechanical properties and fracture behavior, both of which are strongly dependent on microstructure, must be fully considered during the design of a long rod penetrator. Conventional design practices commonly use quasi-static mechanical property values. Modern trends have moved toward characterizing mechanical properties at appropriate dynamic strain rates and implementing them into the design process. Such properties are representative of the dynamic loading conditions associated with the interior (launch), exterior (flight), and terminal ballistic (penetration) phases experienced by a long rod penetrator.

By exploiting the rate sensitivity of WHAs, KE projectiles may be designed using the elevated mechanical properties associated with launch strain rates. This would allow a given subcaliber penetrator to carry more of the launch load and thus reduce sabot mass. From a system perspective, this would present the end user with the choice of (1) using the original penetrator fired at an increased muzzle velocity or (2) substituting a more robust penetrator which could be launched at a comparable velocity to the original rod that was designed to quasi-static mechanical properties. Strain rates on the order of 10^0 to 10^1 s^{-1} are representative of the conditions experienced by long rod penetrators during launch from large-caliber powder cannons. The mechanical properties and fracture behavior of both alloys examined in this report were evaluated in this strain rate regime.

3. MATERIALS

3.1 Alloy Composition and Processing Methods. The weight-percentage compositions of the two commercially available alloys used were 93W-4.9Ni-2.1Fe and 91W-6Ni-3Co. The nominal densities were 17.65 g/cm^3 for the W-Ni-Fe alloy and 17.45 g/cm^3 for the W-Ni-Co material. The W-Ni-Fe alloy was examined in both an as-sintered (and solution heat treated) condition and after swaging and aging. However, the as-sintered material was from a different lot than the one that was swaged and aged. The as-sintered condition provides the basic microstructure of the alloy prior to TM processing. The swaged and aged processing condition for each alloy was selected such that both materials had comparable levels of ductility as measured in terms of quasi-static tensile elongation. Both alloys were swaged by cold-working to a 25% reduction in area, followed by an aging heat treatment for 2 hr at temperature (W-Ni-Fe at 400° C and W-Ni-Co at 500° C).

3.2 Microstructure. Properties and characteristics of a material are based on its microstructure. Consequently, a processing step that alters the properties of a material will change its microstructure. Virgin material samples were sectioned from the ends of the failed tensile specimens, mounted in a clear

medium, and polished for optical microscopy. The microstructure was examined in both the longitudinal (along length of the bar) and transverse (across diameter of the bar) directions. The photomicrographs of the longitudinal and transverse microstructures are shown in Figures 2–7, respectively. Table 1 provides average grain size and contiguity measurements.

The W grains for most as-sintered WHAs are usually spherical in shape. The microstructure of the as-sintered W-Ni-Fe alloy shows a disparity between longitudinal (Figure 2) and transverse (Figure 3) grain size. The grains appear elliptical in the longitudinal direction. This may be due to "slumping" of the W grains, which may have occurred during liquid-phase sintering of this barstock [1]. Note that the matrix is clearly visible between most of the W grains, although some contiguity does exist.

The microstructure of the swaged and aged W-Ni-Fe alloy (Figures 4 and 5) shows that less matrix is visible compared to the as-sintered material. Voids are visible in the matrix and a few W grains, indicating porosity and/or the presence of impurity inclusions. The swaged and aged W-Ni-Co alloy (Figures 6 and 7) has smaller grains, less W-W contiguity, and more binder matrix than the W-Ni-Fe material. Smaller grain size results from a lower sintering temperature. This is consistent with the processing methods used by the manufacturer to make the two materials used in the study, as the W-Ni-Fe alloy was sintered at a higher temperature than W-Ni-Co material [1].

The W grains for both swaged and aged W-Ni-Fe and W-Ni-Co alloys are elongated in the direction of swaging. Bentley and Hogwood have shown that W grains are able to deform (elongate) to almost the same percentage as the applied deformation (up to 30% deformation) [28]. Their work indicates that the increase in longitudinal grain size is accompanied by a decrease in grain size in the transverse direction. A comparison of the change in grain sizes could not be made for the as-sintered and swaged and aged W-Ni-Fe samples because each was from a different lot of material. Yet, a qualitative comparison of grain size ratio (longitudinal W grain size/transverse W grain size) for the swaged and aged alloy shows a reasonable correlation with the results reported by Bentley and Hogwood [26] for a comparable W-Ni-Fe material.

Lower overall W content and a higher W content matrix are responsible for the reduced contiguity and increased volume fraction of matrix in the W-Ni-Co alloy. The W-Ni-Fe binder phase consists of about 24-weight-percent W; whereas, the W-Ni-Co matrix has roughly 38-weight-percent W [1,14]. Small W grains are visible in the W-Ni-Co binder, similar to those observed by Lankford et al. for a comparably

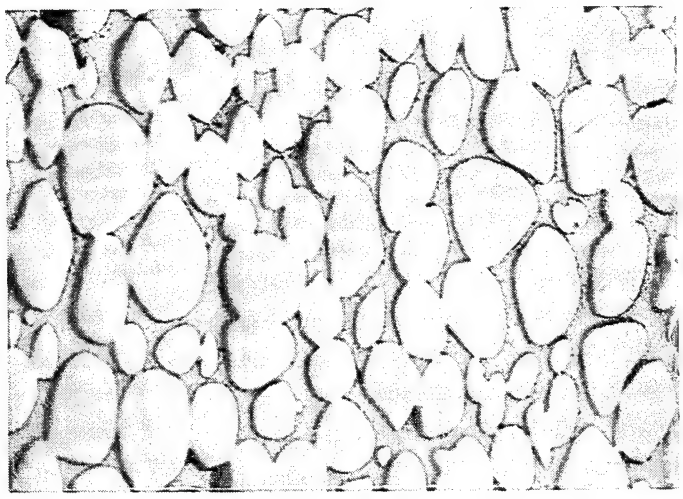

Figure 2. Longitudinal microstructure of as-sintered 93W-4.9Ni-2.1Fe (200×).

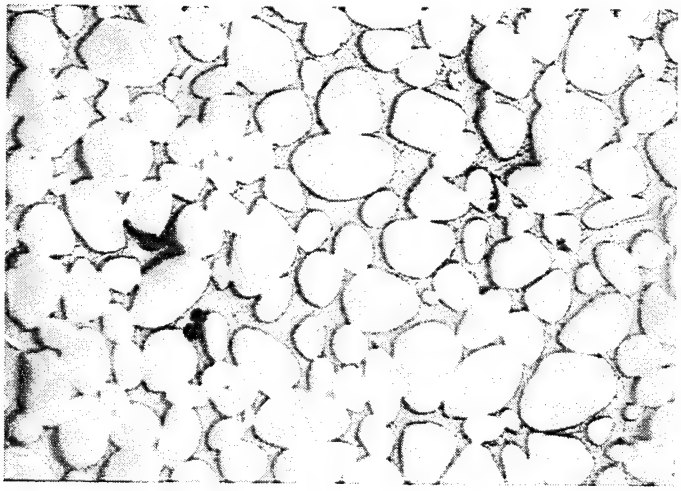

Figure 3. Transverse microstructure of as-sintered 93W-4.9Ni-2.1Fe (200×).

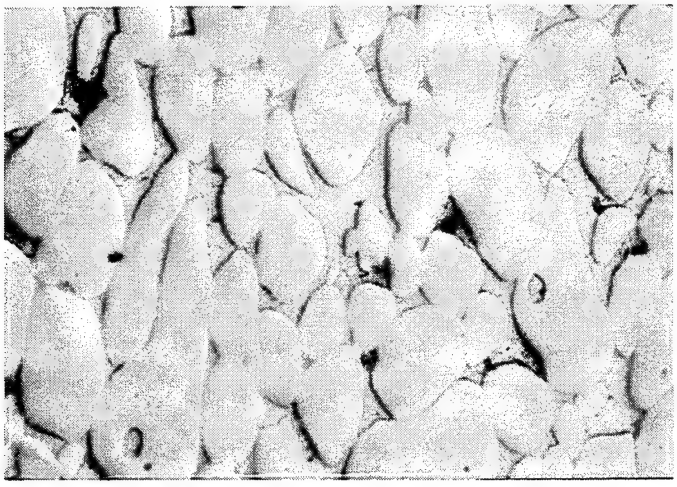

Figure 4. Longitudinal microstructure of swaged and aged 93W-4.9Ni-2.1Fe (200×).

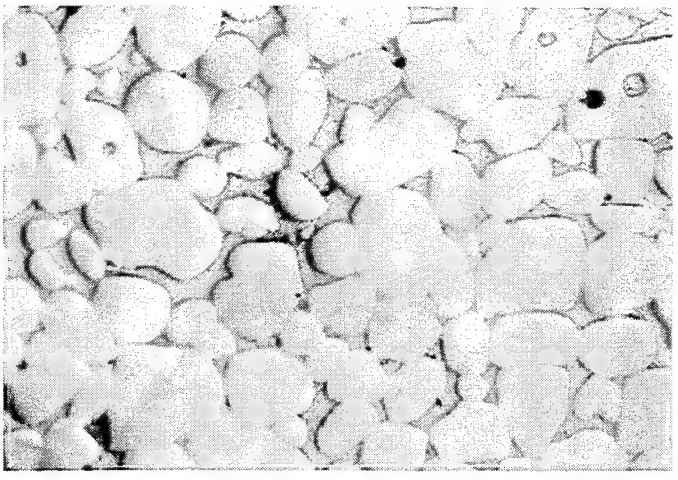

Figure 5. Transverse microstructure of swaged and aged 93W-4.9Ni-2.1Fe (200×).

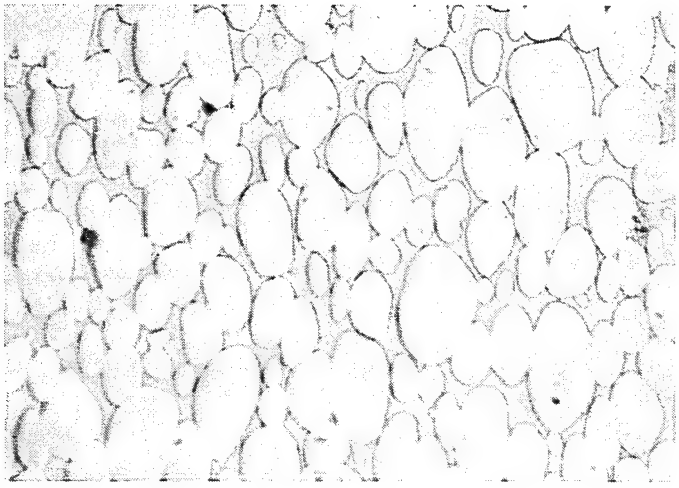

Figure 6. Longitudinal microstructure of swaged and aged 91W-6Ni-3Co (200×).

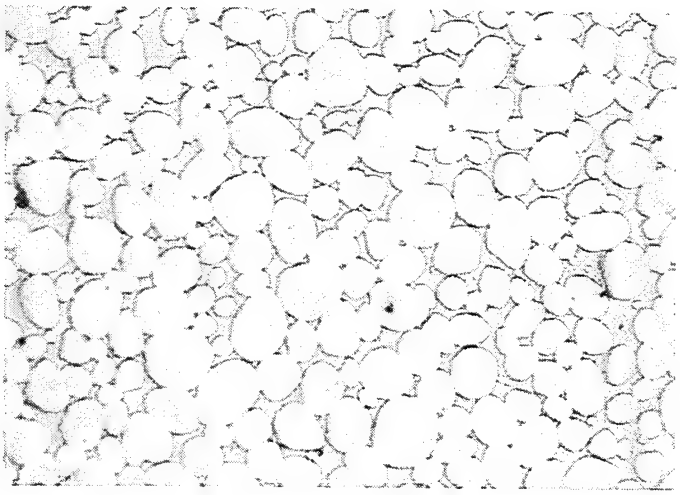

Figure 7. Transverse microstructure of swaged and aged 91W-6Ni-3Co (200×).

Table 1. Grain Size and Contiguity in Longitudinal and Transverse Directions

	Average Grain Size (μm)		Contiguity	
	Longitudinal	Transverse	Longitudinal	Transverse
As-sintered W-Ni-Fe	41	31	.31	.29
Swaged and Aged W-Ni-Fe	49	28	.35	.41
Swaged and Aged W-Ni-Co	36	23	.29	.32

swaged and aged material [3]. Although similar in some aspects, the microstructures of the two alloys are different enough to produce a wide range of mechanical properties. Both alloys have been subjected to an extensive mechanical property characterization [14]. Further discussion concerning the relationship between microstructure and fracture behavior is limited to tensile properties and failures.

3.3 Tensile Properties. Uniaxial tensile tests were performed in the quasi-static ($\dot{\varepsilon} = 10^{-4}$ s^{-1}) and low-to-medium ($\dot{\varepsilon} = 10^{0}$ s^{-1}) strain rate regimes by Dudder [14]. The specimens were right circular cylinders having threaded ends, a 25.4-mm-gauge length, and 6.35-mm-gauge diameter. The results are shown in Table 2. The as-sintered W-Ni-Fe alloy yields at a relatively low value and then work hardens with increasing strain to a modest ultimate tensile strength (UTS) when tested in the quasi-static strain rate regime. This is due to the strain-hardening of the W grains and matrix, although the relative role that each plays is not fully understood [4]. Conversely, when swaged or aged, both alloys yield at much higher stress levels, yet do not exhibit any appreciable strain-hardening. The higher flow stress results from the prior cold-working by swaging and precipitation-strengthening from aging. Note that comparable levels of TM processing produce higher yield strength and UTS values for the W-Ni-Co alloy as compared to W-Ni-Fe. One might expect that the alloy with the overall higher W content would have the higher tensile strength, yet this is not the case. The higher tensile strength of the swaged and aged W-Ni-Co alloy is attributed to the cobalt content as well as increased W in the matrix. This permits both the W grains and the matrix to be work-hardened to higher levels during swaging, which increases the flow stress of the material.

The strain rate dependence of the W heavy alloys becomes evident as the rate of tensile loading is increased from $\dot{\varepsilon} = 10^{-4}$ s^{-1} to $\dot{\varepsilon} = 10^{0}$ s^{-1}. The UTS increases as a function of increasing strain rate for

Table 2. Tensile Properties of W-Ni-Fe and W-Ni-Co Heavy Alloys at 21° C (Dudder 1990)

Strain Rate/Property	As-sintered W-Ni-Fe	Swaged and Aged W-Ni-Fe	Swaged and Aged W-Ni-Co
Quasi-Static ($\dot{\varepsilon} = 10^{-4}$ s^{-1})			
0.2% Yield Strength (MPa)	572	1185	1475
Ultimate Strength (MPa)	896	1206	1509
Reduction in Area (%)	36.3	16.1	14.1
Total Elongation (%)	31.1	9.2	9.6
Low-to-Medium ($\dot{\varepsilon} = 10^{0}$ s^{-1})			
Ultimate Strength (MPa)	1034	1468	1736
Reduction in Area (%)	32.2	6.9	17.6
Total Elongation (%)	21.9	3.8	7.1

each alloy, regardless of processing condition, as shown in Figure 8. Lankford et al. examined the tensile behavior of a similar 25% swaged and aged W-Ni-Co alloy at a dynamic strain rate of 10^3 s^{-1} and observed an even larger increase in UTS [3] as plotted in Figure 8. Note that the UTS for the low-to-medium strain rate falls between the quasi-static and dynamic values.

In terms of ductility, the as-sintered W-Ni-Fe still remains fairly ductile at the low-to-medium strain rate, whereas the W-Ni-Fe alloy (3.8%) has considerably less elongation than the W-Ni-Co material (7.1%) in the swaged and aged condition as shown in Figure 9. This is significant because the W-Ni-Co alloy has the higher UTS. Note also that the dynamic ductility of the W-Ni-Co alloy at $\dot{\varepsilon} = 10^3$ s^{-1} is still at a reasonable level.

The ductility of the W-Ni-Co material at the low-to-medium and dynamic strain rates suggests that a strong interface between W grains and the matrix exists. The integrity of the interface plays a major role in determining the fracture behavior of WHAs. Ductility and fracture behavior are key elements considered by projectile designers during the selection of a penetrator material. Both of these characteristics strongly influence (1) the ability of the projectile to survive launch and (2) the response and performance of a long rod penetrator against targets that impart lateral loads.

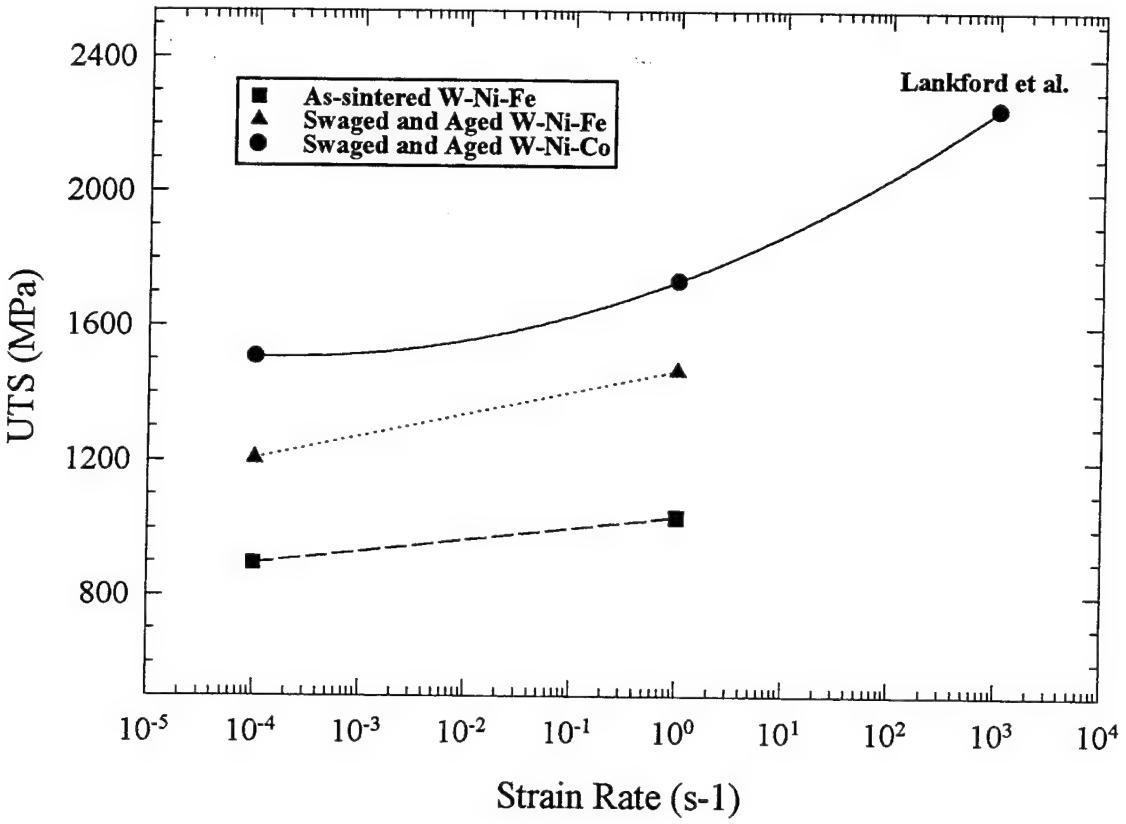

Figure 8. Ultimate tensile strength vs. strain rate (measured at strain to failure).

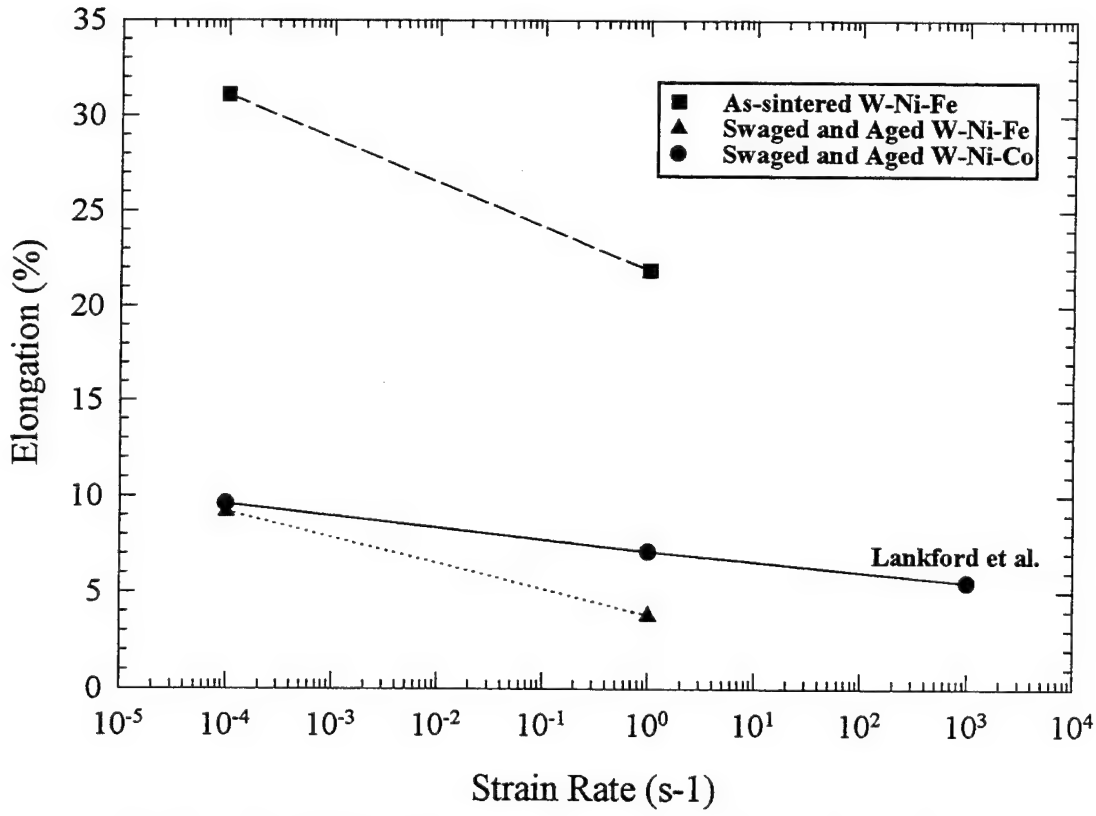

Figure 9. Tensile elongation vs. strain rate (measured at strain to failure).

4. FRACTURE CHARACTERISTICS

The fracture surfaces were characterized using scanning electron microscopy (SEM). Areas of interest included individual W grains, W-W grain boundaries, W-matrix interfaces, and the matrix. SEM photomicrographs indicate that the fracture behavior and tensile properties of the W heavy alloys are strongly influenced by microstructure and rate of loading.

The predominant fracture mode in the quasi-static loading regime, regardless of microstructure, was cleavage of the W grains (Figures 10, 12, and 14). Another failure mode was matrix rupture, particularly for the as-sintered W-Ni-Fe (Figure 10) and swaged and aged W-Ni-Co (Figure 14) alloys. The SEM image of the swaged and aged W-Ni-Fe alloy (Figure 12) reveals partial W-matrix separation, intragranular porosity, and thin areas of matrix between W grains. Note the intragranular crack that has been arrested by the surrounding matrix (middle of Figure 14). Fracture modes of the as-sintered W-Ni-Fe and swaged and aged W-Ni-Co alloys were similar to those observed by Lankford et al. for comparable materials tested in the quasi-static strain rate regime [3].

Fracture behavior of the alloys at the low-to-medium strain rate was characterized by mixed modes of microstructural failure. Intergranular surfaces (W-W facets), which form during separation of contiguous W grains, were observed in each SEM image (Figures 11, 13, and 15) at the higher strain rate. The fracture modes of as-sintered W-Ni-Fe also included matrix rupture and some cleavage of W grains (Figure 11). The large areas of matrix rupture suggest a ductile failure, which was indeed the case as the elongation to failure for the as-sintered material is relatively high at this strain rate.

Intragranular cleavage and fracture, separation of W-W facets, W-matrix decohesion, and isolated matrix rupture are visible for the swaged and aged W-Ni-Fe alloy (Figure 13). Separation of matrix from the W grains led to the nucleation of voids that coalesced as the severity of decohesion increased. The separation of contiguous W-W interfaces and the decohesion between W grains and matrix observed at the higher strain rate were responsible for the low ductility of the W-Ni-Fe alloy. The matrix was incapable of arresting the formation of voids and the intergranular cracks that formed as a result of W-W separation.

The fracture modes for the swaged and aged W-Ni-Co material included intragranular fracture and cleavage, separation of W-W facets, and the rupture of matrix (Figure 15). Note the lack of W-matrix

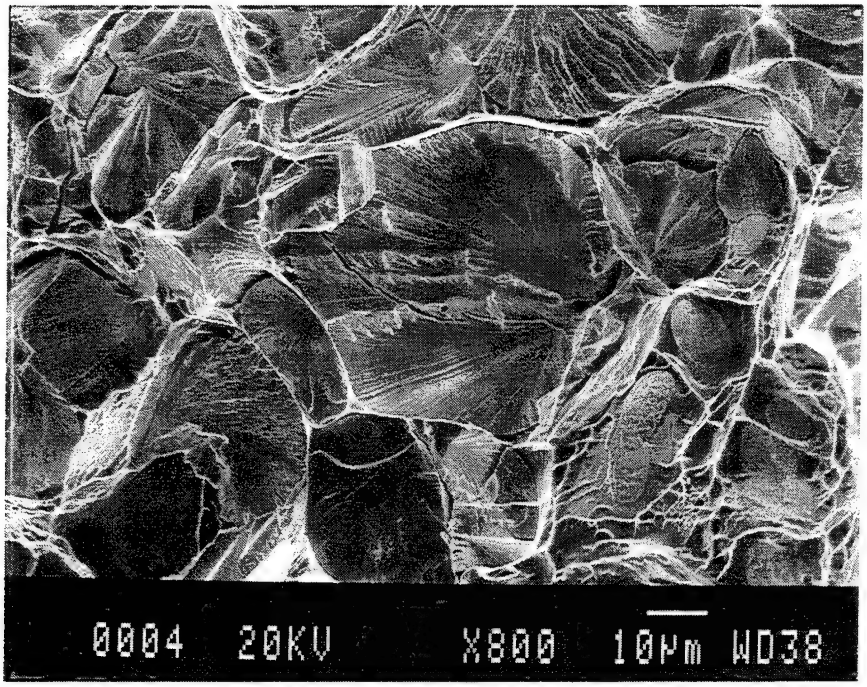

Figure 10. SEM fractograph of as-sintered 93W-4.9Ni-2.1Fe at $\dot{\varepsilon} = 10^{-4}\ s^{-1}$.

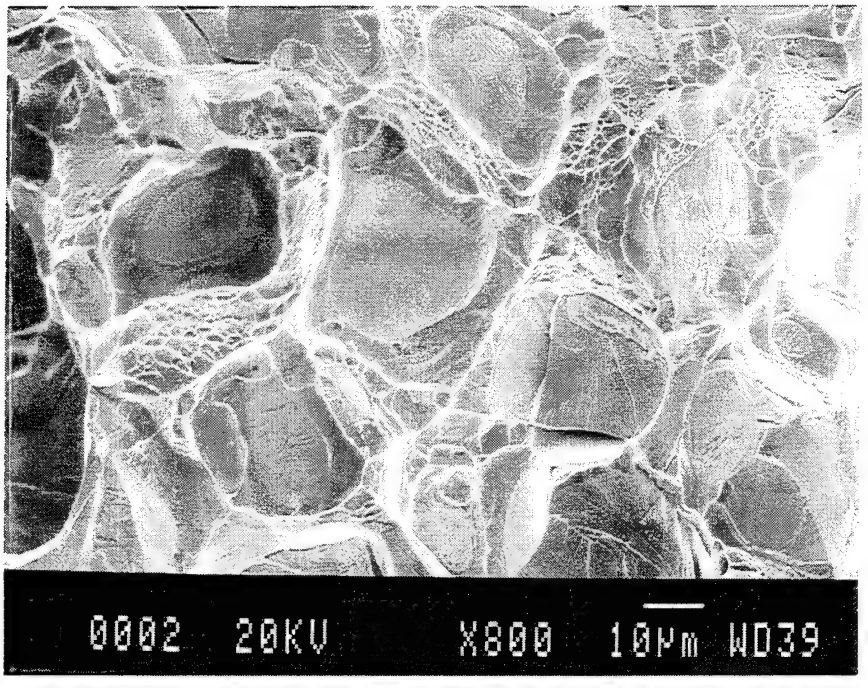

Figure 11. SEM fractograph of as-sintered 93W-4.9Ni-2.1Fe at $\dot{\varepsilon} = 10^{0}\ s^{-1}$.

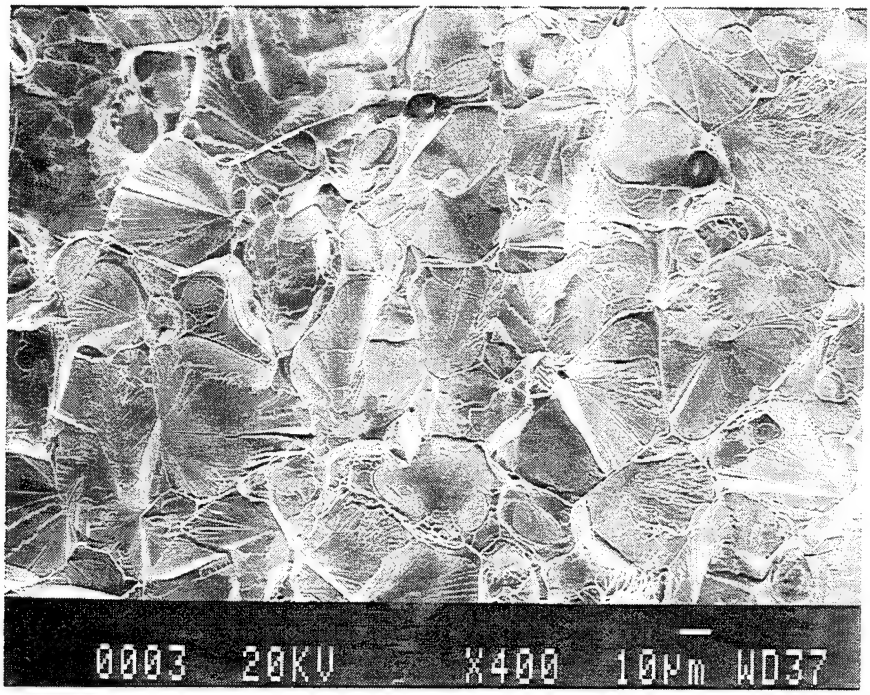

Figure 12. SEM fractograph of swaged and aged 93W-4.9Ni-2.1Fe at $\dot{\varepsilon} = 10^{-4}\ s^{-1}$.

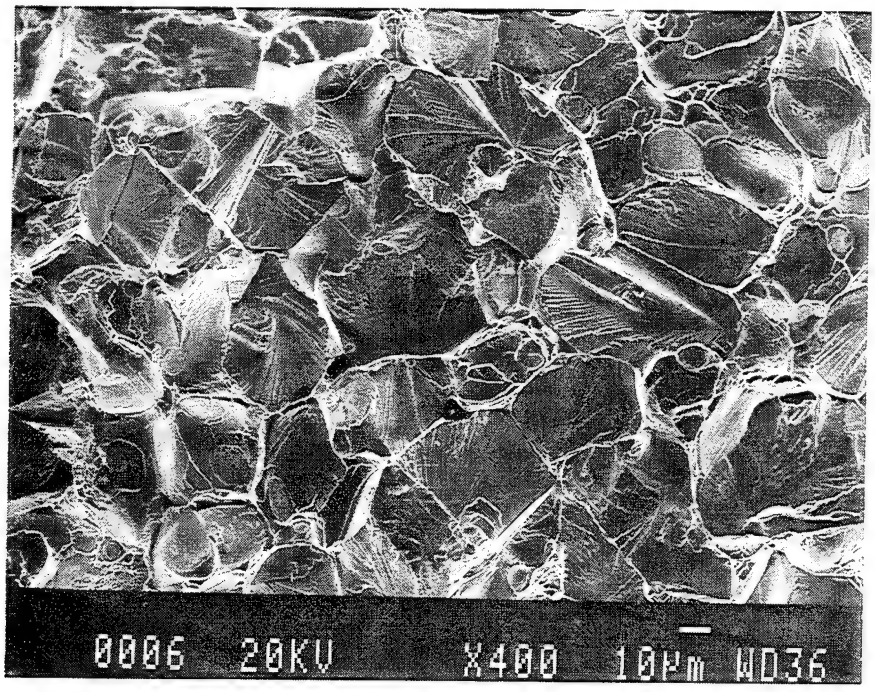

Figure 13. SEM fractograph of swaged and aged 93W-4.9Ni-2.1Fe at $\dot{\varepsilon} = 10^{0}\ s^{-1}$.

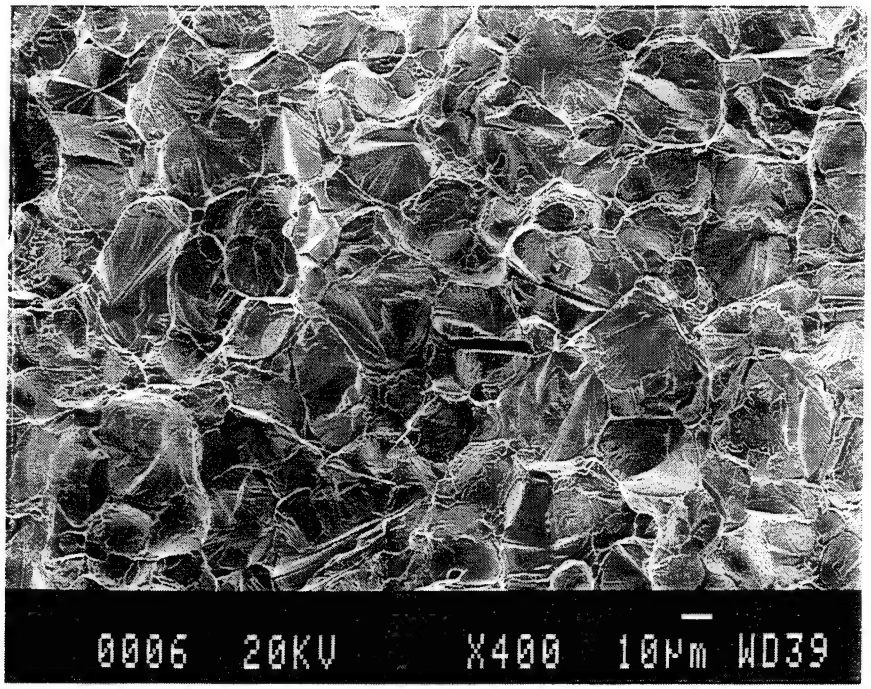

Figure 14. SEM fractograph of swaged and aged 91W-6Ni-3Co at $\dot{\varepsilon} = 10^{-4}\ s^{-1}$.

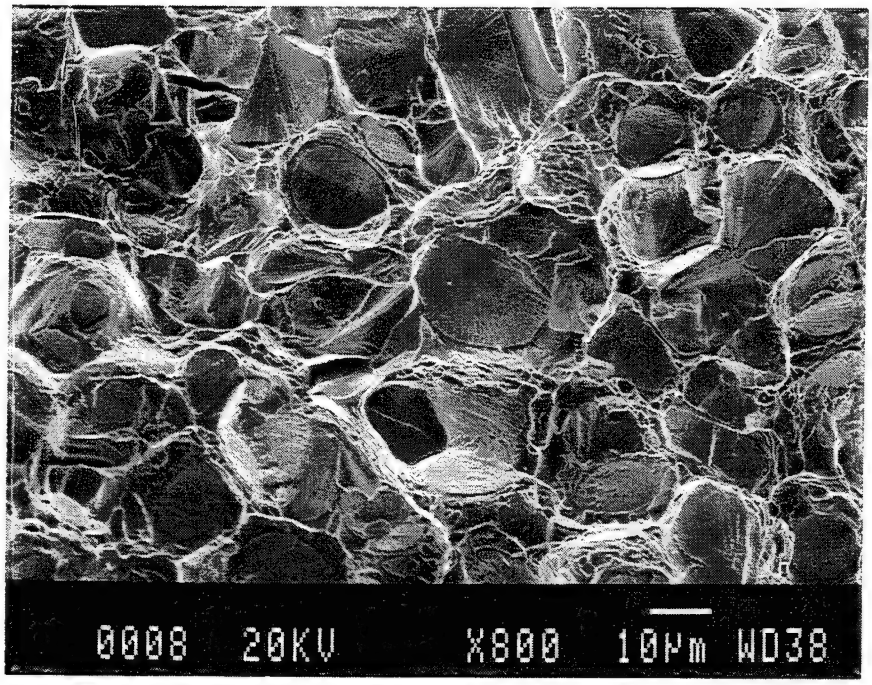

Figure 15. SEM fractograph of swaged and aged 91W-6Ni-3Co at $\dot{\varepsilon} = 10^{0}\ s^{-1}$.

decohesion, indicating that the W-Ni-Co alloy has a strong bond between the matrix and W grains. This may be due to a diffusion mechanism associated with the presence of Co [1]. Good cohesion resulted in a material that was capable of transferring the stresses between W grains and the binder at the higher strain rate without initiating and propagating intergranular cracks. This desirable fracture behavior and a higher UTS value at the low-to-medium strain rate were attributable to increased volume of matrix and increased W and Co content in the matrix of the W-Ni-Co alloy. The fracture behavior of the swaged and aged W-Ni-Co alloy material was qualitatively similar to that observed by Lankford et al. [3] for a comparable alloy tested at a higher strain rate (10^3 s^{-1}). However, quantitative metallography was not performed to determine if the distribution of failure modes was the same at the low-to-medium and dynamic loading rates.

5. CONCLUSIONS

The influence of microstructure and loading rate on the fracture behavior and tensile properties of 93W-4.9Ni-2.1Fe-weight-percent and 91W-6Ni-3Co-weight-percent alloys was investigated. Fracture characteristics of specimens pulled in uniaxial tension at quasi-static ($\dot{\varepsilon}$ = 10^{-4} s^{-1}) and low-to-medium ($\dot{\varepsilon}$ = 10^{0} s^{-1}) strain rates were identified. Failure modes and tensile properties were correlated with respect to microstructure of the two alloys and indicate the following:

(1) For comparable levels of swaging and aging, the 91W-6Ni-3Co alloy had higher tensile strengths than the 93W-4.9Ni-2.1Fe material, indicating that overall W content is not the primary mechanism responsible for increased strength. The W-Ni-Co alloy had more W in the matrix (38 weight-percent) compared to the W-Ni-Fe material (24 weight-percent). The higher volume percentage of matrix, increased weight-percent of W, and presence of Co in the matrix, combined with the smaller average grain size, contributed to enhanced work-hardenability of the W-Ni-Co alloy during swaging, resulting in an effective increase in flow stress. The increase in tensile strength as a function of strain rate was consistent with the results observed for the W-Ni-Co alloy at a higher strain rate of 10^3 s^{-1} [3].

(2) Ductile W grain cleavage was the predominant failure mode for both alloys tested in the quasi-static strain rate regime. Failure at contiguous W-W interfaces and decohesion between W grains and the matrix at the low-to-medium strain rate reduced the ductility

of the swaged and aged W-Ni-Fe alloy. Intergranular fracture readily occurred because the matrix was incapable of preventing void nucleation and coalescence, resulting in crack initiation and growth. Increased volume fraction of a stronger matrix, less W-W contiguity, and better cohesion between matrix and W grains provided the swaged and aged W-Ni-Co alloy with higher strength and ductility at the low-to-medium strain rate. This is a consequence of the more uniform distribution of stress within the material.

Both alloys in the swaged and aged processing condition are suitable for use as KE penetrator materials. Although the as-sintered W-Ni-Fe alloy has high density, excellent ductility, and good fracture characteristics (especially at the low-to-medium strain rate), its low tensile yield strength would require a KE projectile to have a massive sabot to ensure structural integrity of the penetrator during launch. This would add parasitic weight to the projectile and result in a lower muzzle velocity for a given amount of propulsion energy. The swaged and aged W-Ni-Fe alloy is attractive as a long rod penetrator material because of its high density and reasonably high tensile strengths. Yet, the low ductility and dubious fracture characteristics (intergranular fracture and decohesion) at the launch strain rate are not conducive for the design of a lightweight sabot for a long rod penetrator nor to defeat armors that impart large lateral loads. However, the swaged and aged W-Ni-Co alloy possesses superior tensile strengths and ductilities and reasonable fracture characteristics at both the quasi-static and low-to-medium strain rates. This combination makes the W-Ni-Co alloy an excellent candidate for consideration as a long rod KE penetrator material and is also favorable for the design of a minimum mass sabot to launch such a subcaliber, armor-piercing munition.

INTENTIONALLY LEFT BLANK.

6. REFERENCES

1. Caldwell, S. Private communication. Teledyne Firth Sterling, LaVergne, TN, 1992.

2. Doepker, S. P., J. A. Mullendore, and J. R. Spencer. "A Comparison of W-Ni-Fe and W-Ni-Co Heavy Alloys." Tungsten & Tungsten Alloys - 1992, edited by A. Bose and R. J. Dowding. Metal Powder Industries Federation, Princeton, NJ, pp. 273–280, 1993.

3. Lankford, J., A. Bose, H. Couque, and C. E. Anderson. "The Role of Microstructure in the Deformation and Failure of Tungsten Heavy Alloys." Proceedings of Army Symposium on Solid Mechanics, Plymouth, MA, 1991a (submitted).

4. Ramesh, K. T., and R. S. Coates. "Microstructural Influences on the Dynamic Response of Tungsten Heavy Alloys." Metallurgical Transactions A, vol. 23A, pp. 2625–2630, 1992.

5. Rabin, B. H., and R. M. German. "Microstructure Effects on Tensile Properties of Tungsten-Nickel-Iron Composites." Metallurgical Transactions A, vol. 19A, pp. 1523–1532, 1988.

6. O'Donnell, R. G., and R. L. Woodward. "The Composition and Temperature Dependence of the Mechanical Properties of Tungsten Alloys." Metallurgical Transactions A, vol. 21A, pp. 744–748, 1990.

7. Srikanth, V., and G. S. Upadhyaya. "Effect of Cold Work and Annealing on the Mechanical Properties of 90W-7Ni-3Fe Heavy Alloy." Journal of Materials Science Letters, vol. 7, pp. 195–197, 1988.

8. Coates, R. S., and K. T. Ramesh. "The Rate Dependent Deformation of a Tungsten Heavy Alloy." Materials Science and Engineering A, vol. 145, pp. 159–166, 1991.

9. Bourguignon, L. L., and R. M. German. "Sintering Temperature Effects on a Tungsten Heavy Alloy." International Journal of Powder Metallurgy, vol. 24, no. 2, pp. 115–121, 1988.

10. German, R. M., L. L. Bourguignon, and B. H. Rabin. "Microstructure Limitations of High Tungsten Content Heavy Alloys." Journal of Metals, vol. 37, no. 8, pp. 36–39, 1985.

11. Rabin, B. H., A. Bose, and R. M. German. "Characterization of Liquid-Phase Sintered Composite Microstructure." Microstructural Science, edited by M. E. Blum, P. M. French, R. M. Middleton and G. F. Vander Voort, vol. 15, pp. 285–299, Elsevier, NY, 1987.

12. Eisenmann, M. R., and R. M. German. "Property Uniformity in Tungsten Heavy Alloys." Progress in Powder Metallurgy, vol. 38, pp. 203–213, 1983.

13. Eisenmann, M. R., and R. M. German. "Factors Influencing Ductility and Fracture Strength in Tungsten Heavy Alloys." International Journal of Refractory and Hard Metals, vol. 3, pp. 86–91, 1984.

14. Dudder, G. B. Private communication. Battelle Pacific Northwest Laboratory, Richland, WA, 1990.

15. Bose, A., and R. M. German. "Matrix Composition Effects on the Tensile Properties of Tungsten-Molybdenum Heavy Alloys." Metallurgical Transactions A, vol. 21A, pp. 1325–1327, 1990.

16. Spencer, J. R., and J. A. Mullendore. "The Effect of Nickel: Iron Ratios on the Mechanical Properties, Microstructure and Processing of W-Ni-Fe Alloys." Tungsten & Tungsten Alloys - 1992, edited by A. Bose and R. J. Dowding, Metal Powder Industries Federation, pp. 111–118, 1993.

17. Lea, C., C. Muddle, and D. V. Edmonds. "Segregation to Interphase Boundaries in Liquid-Phase Sintered Tungsten Alloys." Metallurgical Transactions A, vol. 14A, pp. 667–677, 1983.

18. Dudder, G. B., and W. E. Gurwell. "Hydrogen Embrittlement Effects on Tensile Properties of Tungsten Heavy Alloys." Tungsten and Tungsten Alloys-Recent Advances, edited by A. Crowson and E. S. Chen, TMS, Warrendale, PA, pp. 161–167, 1991.

19. Woodward, R. L., and R. G. O'Donnell. "Microstructural Influences on the Ductility of Tungsten Alloys." Tungsten & Tungsten Alloys - 1992, edited by A. Bose and R. J. Dowding, Metal Powder Industries Federation, Princeton, NJ, pp. 273–280, 1993.

20. Churn, K. S., and R. M. German. "Fracture Behavior of W-Ni-Fe Heavy Alloys." Metallurgical Transactions A, vol. 15A, pp. 331–338, 1984.

21. Lankford, J., H. Couque, A. Bose, and R. German. "Dynamic Deformation and Failure of Tungsten Heavy Alloys." Tungsten and Tungsten Alloys-Recent Advances, edited by A. Crowson and E. S. Chen, TMS, Warrendale, PA, pp. 151–159, 1991.

22. Couque, H., and J. Lankford. "Influence of Loading Rate on Fracture Properties of Heavy Metals." Mechanical Properties of Materials at High Rates of Strain, Institute of Physics Conference Series No. 102, pp. 227–236, The Institute of Physics, Bristol, England, 1989.

23. Drysdale, W. H. "Design of Kinetic Energy Projectiles for Structural Integrity." BRL-TR-02365, U.S. Army Ballistic Research Laboratory, Aberdeen Proving Ground, MD, September 1981.

24. Sorensen, B. R. "Implementation of a CAD/CAM System to Design, Analyze, and Manufacture Prototype Kinetic Energy Projectiles." BRL-TR-3272, U.S. Army Ballistic Research Laboratory, Aberdeen Proving Ground, MD, October 1991.

25. Sorensen, B. R. "Design and Analysis of Kinetic Energy Projectiles Using Finite Element Optimization." BRL-TR-3289, U.S. Army Ballistic Research Laboratory, Aberdeen Proving Ground, MD, November 1991.

26. Magness, L. S., and T. G. Farrand. "Deformation Behavior and Its Relationship to the Penetration Performance of High-Density KE Penetrator Materials." Proceedings of 1990 Army Science Conference, Durham, NC, pp. 149–164, May 1990.

27. Leonard, W., L. Magness, and D. Kapoor. "Ballistic Evaluation of Thermo-Mechanically Processed Tungsten Heavy Alloys." BRL-TR-3326, U.S. Army Ballistic Research Laboratory, Aberdeen Proving Ground, MD, April 1992.

28. Bentley, A. R., and M. C. Hogwood. "Effect of Mechanical Deformation and Heat Treatment on the Microstructural Characteristics of Two Tungsten Heavy Alloys." Tungsten & Tungsten Alloys - 1992, edited by A. Bose and R. J. Dowding. Metal Powder Industries Federation, Princeton, NJ, pp. 419–430, 1993.

INTENTIONALLY LEFT BLANK.

NO. OF COPIES	ORGANIZATION
2	DEFENSE TECHNICAL INFO CTR ATTN DTIC DDA 8725 JOHN J KINGMAN RD STE 0944 FT BELVOIR VA 22060-6218
1	DIRECTOR US ARMY RESEARCH LAB ATTN AMSRL OP SD TA 2800 POWDER MILL RD ADELPHI MD 20783-1145
3	DIRECTOR US ARMY RESEARCH LAB ATTN AMSRL OP SD TL 2800 POWDER MILL RD ADELPHI MD 20783-1145
1	DIRECTOR US ARMY RESEARCH LAB ATTN AMSRL OP SD TP 2800 POWDER MILL RD ADELPHI MD 20783-1145
	ABERDEEN PROVING GROUND
5	DIR USARL ATTN AMSRL OP AP L (305)

NO. OF COPIES	ORGANIZATION
1	HQDA ATTN SARD TT F MILTON WASHINGTON DC 20310-0103
1	DIRECTOR ATTN JAMES RICHARDSON ADV RSRCH PROJECTS AGENCY 3701 N FAIRFAX DR ARLINGTON VA 22203-1714
2	COMMANDER ATTN AMSMI RD ST WF D LOVELACE M SCHEXNAYDER US ARMY MICOM REDSTONE ARSENAL AL 35898-5250
2	PROGRAM MANAGER ATTN SSAE AR TMA CARL ROLLER ROBERT KOWALSKI TANK MAIN ARMAMENTS SYSTEMS PICATINNY ARSENAL NJ 07806-5000
2	COMMANDER ATTN AMSTA AR AET M DEEPAK KAPOOR SHELDON CYTRON BLDG 355 US ARMY ARDEC PICATINNY ARSENAL NJ 07806-5000
5	COMMANDER ATTN AMSTA AR CCH A NICK KRASNOW PAUL CHRISTIAN MARTY CONNER SAIF MUSALLI RAY CARR US ARMY ARDEC PICATINNY ARSENAL NJ 07806-5000
1	COMANDER ATTN AMSTA AR RENATA PRICE US ARMY ARDEC PICATINNY ARSENAL NJ 07806-5000
1	COMMANDER ATTN AMSTA AR CC JOHN HEDDERICH US ARMY ARDEC PICATINNY ARSENAL NJ 07806-5000
1	AIR FORCE ARMAMENT LAB ATTN TECHNICAL LIBRARY EGLIN AFB FL 32542
1	COMMANDER ATTN TECHNICAL LIBRARY NAVAL WEAPONS CENTER CHINA LAKE CA 93555
4	DIRECTOR ATTN HASKELL SHEINBERG PAUL DUNN BILLY HOGAN DON RABERN LOS ALAMOS NATIONAL LAB PO BOX 1663 G770 LOS ALAMOS NM 87545
3	OSRAM SYLVANIA INC ATTN JAMES SPENCER JAMES MULLENDORE SUSAN DOEPKER HAWES ST TOWANDA PA 18848
1	PARMATECH CORPORATION ATTN ANIMESH BOSE 2221 PINE VIEW WAY PETALUMA CA 94954
1	TELEDYNE ADVANCED MATERIALS ATTN STEVEN CALDWELL #1 TELEDYNE PLACE LAVERGNE TN 37086
1	PENNSYLVANIA STATE UNIVERSITY ATTN RANDALL M GERMAN 118 RESEARCH BLDG WEST UNIVERSITY PARK PA 16802-6809
3	BATTELLE PACIFIC NORTHWEST LAB ATTN BILL GURWELL GORDON DUDDER RAY SHIPPELL PO BOX 999 RICHLAND WA 99352

NO. OF COPIES	ORGANIZATION
4	OLIN CORPORATION ATTN DEL ROD ED STEINER TOM MCGOVERN TOM LYNCH FLINCHBAUGH DIV 200 E HIGH ST PO BOX 127 RED LION PA 17356
1	CONCURRENT TECH CORP ATTN TIMOTHY MCCABE 1450 SCALP AVE JOHNSTOWN PA 15904
2	SOUTHWEST RSRCH INSTITUTE ATTN CHARLES ANDERSON JAMES LANKFORD PO DRAWER 28510 SAN ANTONIO TX 78228-0510
3	INSTITUTE FOR ADVANCED TECH ATTN STEPHAN BLESS THOMAS KIEHNE RAVI SUBRAMANIAN UNIV OF TEXAS - AUSTIN 4030-2 W BRAKER LANE AUSTIN TX 78759
3	GENERAL RSRCH CORP ATTN WILLIAM ISBELL THOMAS MENNA CHRIS PACE 5383 HOLLISTER AVE SANTA BARBARA CA 93160
1	SANDIA NATIONAL LAB ATTN DENNIS GRADY DEPT 1433 MS 0821 ALBUQUERQUE NM 87185
1	SANDIA NATIONAL LAB ATTN MARLIN KIPP DEPT 1431 MS 0820 ALBUQUERQUE NM 87185
1	PROJECT MANAGER ATTN SFAE MS LS EM BRIAN SABOURIN LINE OF SIGHT ANTITANK REDSTONE ARSENAL AL 35989-8000

NO. OF COPIES	ORGANIZATION
1	THE JOHNS HOPKINS UNIV ATTN K T RAMESH DEPT OF MECHANICAL ENG 3400 N CHARLES ST BALTIMORE MD 21218
3	DIRECTOR ATTN C CLINE R GOGOLEWSKI J REAUGH LAWRENCE LIVERMORE NATL LAB BOX 808 LIVERMORE CA 94550
4	ALLIANT TECHSYSTEMS ATTN GORDON JOHNSON CAL CANDLAND MITCH DANIELSON (MN 2881) TIM HOLMQUIST (MN 2720) 600 SECOND ST NE HOPKINS MN 55343
2	TITAN RSRCH & TECH CORP ATTN ROLAND FRANZEN DENNIS ORPHAL 5117 JOHNSON DR PLEASANTON CA 94566
1	KAMAN SCIENCES CORP ATTN STEVE DIEHL 1500 GARDEN OF THE GODS RD PO BOX 7463 COLORADO SPRINGS CO 80933
1	LORAL VOUGHT SYSTEMS ATTN ROGER MELIN PO BOX 650003 M S SP 52 DALLAS TX 75265-0003

NO. OF COPIES ORGANIZATION

ABERDEEN PROVING GROUND

55 DIR USARL
ATTN AMSRL MA CB
ROBERT DOWDING
PATRICK WOOLSEY
AMSRL WT
D. ECCLESHALL
AMSRL WT PB
E. SCHMIDT
AMSRL WT PD
B. BURNS
W. DRYSDALE
AMSRL WT T
W. MORRISON
T. WRIGHT
AMSRL WT TA
W. GILLICH
T. HAVEL
W. BRUCHEY
M. BURKINS
E. RAPACKI
W. GOOCH
D. HACKBARTH
M. ZOLTOSKI
M. KEELE
S. BILYK
G. FILBEY
J. DEHN
E. HORWATH
G. BULMASH
H. MEYER
Y. HUANG
N. RUPERT
W. ROWE
J. RUNYEON

NO. OF COPIES ORGANIZATION

AMSRL WT TC
W. DE ROSSET
L. MAGNESS
R. COATES
K. KIMSEY
D. SCHEFFLER
W. WALTERS
R. SUMMERS
F. GRACE
T. BJERKE
B. SORENSEN
R. MUDD
W. WALTERS
M. LAMPSON
F. MALINOSKI
A. COPLAND
G. SILSBY
R. PHILLABAUM
E. KENNEDY 4 CPS
AMSRL WT TD
S. SEGLETES
K. FRANK
D. DIETRICH
P. KINGMAN
T. FARRAND
AMSRL WT WD
L. KECSKES
AMSRL WT WE
J. TEMPERLEY

NO. OF COPIES	ORGANIZATION
2	COMMANDER DRA FORT HALSTEAD ATTN MICHAEL HOGWOOD ALISON BENTLEY SEVENOAKS KENT TN14 7BP ENGLAND UNITED KINGDOM
1	DIRECTOR MATERIALS RSRCH LAB ATTN R WOODWARD P.O. BOX 50 ASCOT VALE, VIC 3052 AUSTRALIA
1	DIRECTOR DEFENCE RSRCH ESTABLISHMENT VALCARTIER ATTN W. ROBERTSON P.O. BOX 8800 COURCELLETTE, QUEBEC G0A 1R0 CANADA
1	L'INGENIEUR EN CHEF DE L'ARMAMENT CHARTIER CENTRE TECHNIQUE ARMES ET MUNITIONS ETABLISSEMENT TECHNIQUE DE BOURGES CARREFOUR DE ZERO-NORD -ROUTE DE GUERRY BP 712 18015 BOURGES CEDEX FRANCE

INTENTIONALLY LEFT BLANK.

USER EVALUATION SHEET/CHANGE OF ADDRESS

This Laboratory undertakes a continuing effort to improve the quality of the reports it publishes. Your comments/answers to the items/questions below will aid us in our efforts.

1. ARL Report Number ARL-MR-269 Date of Report November 1995

2. Date Report Received _____

3. Does this report satisfy a need? (Comment on purpose, related project, or other area of interest for which the report will be used.) _____

4. Specifically, how is the report being used? (Information source, design data, procedure, source of ideas, etc.) _____

5. Has the information in this report led to any quantitative savings as far as man-hours or dollars saved, operating costs avoided, or efficiencies achieved, etc? If so, please elaborate. _____

6. General Comments. What do you think should be changed to improve future reports? (Indicate changes to organization, technical content, format, etc.) _____

CURRENT ADDRESS

_____
Organization

_____
Name

_____
Street or P.O. Box No.

_____
City, State, Zip Code

7. If indicating a Change of Address or Address Correction, please provide the Current or Correct address above and the Old or Incorrect address below.

OLD ADDRESS

_____
Organization

_____
Name

_____
Street or P.O. Box No.

_____
City, State, Zip Code

(Remove this sheet, fold as indicated, tape closed, and mail.)

(DO NOT STAPLE)